

Supplementary Materials for  
**Structural and mechanistic basis of neutralization by a pan-hantavirus  
protective antibody**

Eva Mittler *et al.*

Corresponding author: Felix A. Rey, felix.rey@pasteur.fr; Andrew S. Herbert, andrew.s.herbert4.civ@health.mil;  
Laura M. Walker, laurawalker410@gmail.com; Kartik Chandran, kartik.chandran@einsteinmed.edu;  
Pablo Guardado-Calvo, pablo.guardado-calvo@pasteur.fr

*Sci. Transl. Med.* **15**, eadg1855 (2023)  
DOI: 10.1126/scitranslmed.adg1855

**The PDF file includes:**

Materials and methods  
Figs. S1 to S16  
Table S1  
Legends for data files S1 and S2  
References (40–62)

**Other Supplementary Material for this manuscript includes the following:**

Data files S1 and S2  
MDAR Reproducibility Checklist

## **MATERIALS AND METHODS**

### **Cell lines**

African green monkey kidney Vero [American Type Culture Collection (ATCC) Cat# CCL-81] and VeroE6 cells (ATCC Cat# CRL-1586) were cultured in a humidified incubator at 37°C with 5% CO<sub>2</sub> in high-glucose Dulbecco's modified Eagle medium (DMEM, Life Technologies) supplemented with 2% fetal bovine serum (FBS, Atlanta Biologicals), 1% GlutaMAX, and 1% penicillin-streptomycin (both Life Technologies). Human hepatocarcinoma Huh.7.5.1 cells (a generous gift of J. Carette, Stanford University) were maintained in high-glucose DMEM (Life Technologies) supplemented with 10% FBS (Atlanta Biologicals), 1% GlutaMAX (Life Technologies), 1% non-essential amino acids (Life Technologies) and 1% penicillin-streptomycin (Life Technologies). Human umbilical vein endothelial cells (HUVECs, Invitrogen, Cat# C0035C) were maintained in human large vessel endothelial (LVE) cell basal medium (Invitrogen, Cat# M-200-500) supplemented with LVE supplements (Invitrogen, Cat# A14608-01) at 37°C with 5% CO<sub>2</sub>. Alternatively, HUVECs (ATCC, Cat# CRL-1730) were maintained in endothelial cell growth medium (Lonza, Cat# CC-3156) supplemented with endothelial cell growth medium-2 SingleQuots (Lonza, Cat# CC-4176) at 37°C with 5% CO<sub>2</sub>. Freestyle 293-F cells (Thermo Fisher Scientific, Cat# R79007) were grown in FreeStyle 293 expression media, at 37°C with 8% CO<sub>2</sub> in a shaking incubator. Mygla.REC.B bank vole epithelial cells (a gift of I. Eckerle, Geneva Centre for Emerging Viral Diseases) were cultured as described previously (40). *Drosophila melanogaster* S2 cells (Thermo Fisher Scientific, Cat# R69007) were maintained in serum-free insect cell medium (HyClone, GE Healthcare) supplemented with 1% penicillin-streptomycin in spinner flasks in a 28°C humidified shaking incubator. Chinese hamster ovary (FreeStyle CHO-S) cells (Gibco, Cat# R80007) were cultured in a humidified incubator at 37°C with 5% CO<sub>2</sub> in CHOgro expression media (Mirus Bio, Cat# MIR 6200).

### **Recombinant Vesicular Stomatitis Virus (rVSV) engineering and neutralization assays**

rVSVs expressing enhanced green fluorescent protein (eGFP) and bearing Gn/Gc from Hantaan virus (HTNV), Seoul virus (SEOV), Dobrava-Belgrade virus (DOBV), Andes virus (ANDV), Sin Nombre virus

(SNV), Choclo virus (CHOV) or chikungunya virus (CHIKV) E3-E2-6K-E1 protein from the African prototype S27 strain (UniProt Accession no. Q8JUX5) were engineered, rescued and propagated following published protocols (9, 41–45). rVSV carrying a phosphoprotein fused to mNeonGreen (mNG) and bearing Puumala virus (PUUV) Gn/Gc has been described previously (46). Generation of viruses with an equivalent eGFP backbone decorated with Laguna Negra virus (LANV) Gn/Gc (GenBank code AF005728) was performed by using standard molecular biology techniques. The identity and sequence of each virus-encoded Gn/Gc was determined by Sanger sequencing of rVSV genomic RNA-derived cDNAs. All viruses were propagated on Vero cells except rVSV-PUUV-Gn/Gc, which was amplified on Huh.7.5.1 cells. Infectivity measurements and neutralization assays on confluent Vero cells with pre-titrated amounts of pseudotyped rVSV particles bearing either PUUV, HTNV, SEOV, DOBV, ANDV, SNV, CHOV, or LANV Gn/Gc or, when indicated, rVSV-ANDV, and -SNV-Gn/Gc neutralization-escape mutants were performed as described previously (20). Infected (eGFP+ or mNG+) cells were automatically counted using a Cytation 5 cell imaging multi-mode reader (BioTek Instruments) or a Cell-Insight CX5 imager (Thermo Fisher) including onboard software. Virus neutralization data were subjected to nonlinear regression analysis to derive half-maximal inhibitory concentration (IC<sub>50</sub>) values using a 4-parameter, variable slope sigmoidal dose-response equation constraining bottom parameters to 0-100 (GraphPad Prism).

### **Authentic virus infections and neutralization assays**

PUUV strain Suonenjoki (PUUV/Suo) was propagated in Mygla.REC.B bank vole epithelial cells (40), whereas PUUV strain Kazan was grown in VeroE6 cells as described (47). VeroE6 cells were exposed to PUUV strain Kazan at a multiplicity of infection (MOI) of 0.1 to 1 of fluorescent focus-forming units (FFU) after a pre-incubation with indicated monoclonal antibody (mAb) concentrations. Viral infectivity was calculated by immunostaining of formaldehyde-fixed cells at 24 hours after infection using polyclonal rabbit serum targeting the PUUV nucleocapsid (N) protein (BEI Resources, Cat# NR-9675). Plates were imaged with the Plate RUNNER HD (Trophos) and images were analyzed, and individual infected cells counted using the system's onboard software.

ANDV strain Chile-9717869 used for in vitro microneutralization assays was propagated and viral titers determined using VeroE6 cells as previously described (41, 48). For neutralization assays, pre-titrated amounts of virus were mixed with serially diluted mAbs for 1 hour before adding virus-mAb mixture to HUVECs at an MOI of 0.5. Viral infectivity was determined by immunostaining of formaldehyde-fixed and permeabilized cells at 48 hours after infection with polyclonal rabbit serum specific for ANDV N protein (BEI Resources, Cat# NR-9673). Images were acquired on an Operetta high-content imaging device (PerkinElmer). Images were analyzed with a customized scheme built from image analysis functions present in the Harmonia software, and the percentage of infected cells was determined using the analysis functions.

For in vitro focus-reduction neutralization assays, 50 to 100 FFUs of ANDV strain Chile-7913 were mixed with serially diluted mAbs for 1 hour before adding virus-mAb mixture to VeroE6 cells. Mixtures were removed after an incubation of 2 hours at 37°C, cells washed with phosphate-buffered saline (PBS), covered with an overlay medium [equal volumes of 2.4% methylcellulose and 2X Eagle's Minimum Essential Medium (Gibco) supplemented with 5% FBS and 2X penicillin-streptomycin (Life Technologies)] and incubated at 37°C for 7 days. Overlay was removed and viral infectivity was determined by immunostaining of methanol-fixed cells with polyclonal rabbit sera specific for ANDV N protein. The number of foci were counted by hand on a CKX53 microscope (Olympus LS). Virus neutralization data were subjected to nonlinear regression analysis to derive IC<sub>50</sub> values using a four-parameter, variable slope sigmoidal dose-response equation constraining bottom parameters to 0 to 100 (GraphPad Prism).

Zika virus (ZIKV) strain MR766 (ATCC, Cat# VR-84) was propagated in Vero cells. For in vitro neutralization assays, Vero cells were exposed to pre-titrated amounts of ZIKV after a pre-incubation with indicated concentrations of ADI-42898. Viral infectivity was determined by immunostaining of formaldehyde-fixed cells at 36 hours after infection using a pan-flavivirus mouse mAb, 4G2 (EMD Millipore, Cat# MAB10216). Infected cells were automatically enumerated using a Cytation 5 cell imaging multi-mode reader (BioTek Instruments) including the system's onboard software.

### **Authentic hantavirus plaque assays**

Confluent monolayers of VeroE6 cells on 6-well plates were aged for 7 to 10 days at 37°C and 5% CO<sub>2</sub> and then inoculated with serial dilutions of virus prepared in minimum essential media (MEM) supplemented with 5% FBS, 2 mM L-glutamine and 1% gentamicin. After adsorption for 1 hour at 37°C, monolayers were overlaid with Eagle basal medium (EBME) supplemented with 0.5% agarose (Seakem), 30 mM Hepes buffer, and 5% FBS. After incubation at 37°C for additional 7 days, a second overlay, supplemented with 5% Neutral red, was added. Plates were removed from the incubator on day 9 and allowed to sit at room temperature for 24 hours protected from light. Plaques were counted the following day and titers were expressed as plaque-forming units (PFU)/ml.

### **Selection of rVSV neutralization-escape mutants**

Selection of escape mutants was performed as described previously (32). In short, rVSV-ANDV-Gn/Gc and rVSV-SNV-Gn/Gc were pre-incubated with a concentration of ADI-42898 corresponding to its 90% inhibitory concentration (IC<sub>90</sub>) value derived from neutralization assays, and then added to confluent monolayers of Vero cells. Supernatants were harvested and following several serial passages under mAb selection, supernatants were tested for viral neutralization escape. If resistance was evident, individual viral clones were plaque-purified on Vero cells, and their Gn/Gc-encoding sequences were determined.

### **Preparation of virus-like particles (VLPs)**

Open-reading frames encoding C-terminally flag-tagged ANDV Gn/Gc or PUUV Gn/Gc were cloned into an expression plasmid (pCAGGS) under the control of a human cytomegalovirus (HCMV) promoter. Plasmids were transfected into FreeStyle 293-F cells with polyethylenimine (Polysciences) and cells were grown for 72 hours. Cell supernatant was clarified and passed through an 0.45-µm pore filter. VLPs were purified by ultracentrifugation at 23,600 rpm for 75 minutes in an SW28 rotor, resuspended in NT buffer [10 mM Tris-HCl (pH 7.5), 135 mM NaCl] and stored at -80°C.

### **Expression and purification of recombinant Gn<sup>H</sup>/Gc**

To obtain the PUUV Gn<sup>H</sup>/Gc complex (strain Mu/07/1219, GenBank code AJC50718 (49)), we followed the approach described previously (15). In short, we generated a codon-optimized DNA fragment for expression in *Drosophila melanogaster* S2 cells encoding Gn<sup>H</sup> [amino acid residues (aa) 20 to 381] in frame with the Gc ectodomain (aa 659 to 1093). Both subunits were joined using a linker (GGSGLVPRGSGGGSGGG**SWHPQFEK**GGGTGGGTLVPRGSGTGG) containing two thrombin cleavage sites (underlined) at either end and a Strep-tag sequence in the middle (bold). Gn<sup>H</sup>/Gc encoding sequences were inserted into a modified pMT/BiP plasmid (Invitrogen) expressing them in frame with a C-terminal double Strep-tag. This plasmid was used to generate stable *Drosophila melanogaster* S2 cells, which were selected and maintained in spinner-flasks in serum-free insect cell medium containing puromycin (7 µg/ml). Recombinant protein expression was induced by adding 5 µM CdCl<sub>2</sub> and cell supernatant was harvested 5 days after induction, supplemented with avidin (10 µg/ml) and 0.1 M Tris-HCl (pH 8.0). Proteins were purified to homogeneity by Strep-Tactin affinity chromatography, followed by size exclusion chromatography (SEC) using a Superdex 200 10/30 column (GE Healthcare) in a buffer composed of 10 mM Tris-HCl (pH 8), 150 mM NaCl, and 1 mM EDTA.

We produced the ANDV Gn<sup>H</sup>/Gc complex (strain Chile-9717869, NCBI code NP\_604472.1) using a protocol described elsewhere (15). The protein was purified using affinity and size exclusion chromatography from the supernatants of stable *Drosophila melanogaster* S2 cells. The protein thus purified is in equilibrium between a main fraction composed of a monomeric form, and a minor fraction composed of its dimeric form, as assessed by size exclusion chromatography coupled to multi-angle light scattering (SEC-MALS).

### **Expression and purification of IgGs, single-chain variable (scFv) fragments and Fab fragments**

Full-length IgG1 proteins used for initial in vitro assays as well as germline-reverted (IGL) mAb constructs, WT:IGL chimeras and variants of ADI-42898 with nucleotide mutations were expressed in *Saccharomyces cerevisiae* cultures, as previously described (50). Briefly, yeast cultures were grown in 24-well plates in a

shaking incubator at 30°C. After 6 days, the culture supernatants were harvested by centrifugation, and IgGs were purified by protein A affinity chromatography. Bound IgGs were eluted [200 mM acetic acid, 50 mM NaCl (pH 3.5)] and buffer-exchanged into PBS, pH 7.0. Fab fragments were generated by digesting IgGs with papain for 2 hours at 30°C, the reaction was terminated by the addition of iodoacetamide and passed over protein A agarose to remove Fc fragments and undigested IgG. The flow-through of the protein A agarose was passed over KappaSelect resin (Cytiva) and Fabs were eluted [200 mM acetic acid, 50 mM NaCl (pH 5.2)] into 1/8 volume of 2 M HEPES buffer (pH 8.0). To generate scFv fragments of ADI-42898, sequences encoding the heavy chain variable region ( $V_H$ ) and light chain variable region ( $V_L$ ) were joined together by a flexible (GS) linker and cloned into a modified pMT/BiP plasmid (Invitrogen). The antibody fragments were purified following the protocol described above in the “Expression and purification of recombinant  $Gn^H/Gc$ ” section.

For authentic hantavirus neutralization assays, *in vivo* protection studies, and antibody biophysical characterizations, mAbs were produced as full-length IgG1 proteins in FreeStyle CHO-S cells as previously described (51). Briefly, the  $V_H$ - and  $V_L$ -encoding sequences were inserted into vectors encoding human heavy chain (HC) and light chain (LC) constant regions and transiently transfected into CHO-S cells. After 6 days, the IgG-containing supernatants were harvested by centrifugation and purified by protein A affinity chromatography. Bound IgGs were eluted, further purified by SEC to at least 95% purity and buffer-exchanged into 150 mM NaCl supplemented with 20 mM histidine (pH 6.0).

### **Crystallization and structure determination**

The complex between PUUV  $Gn^H/Gc$  and the ADI-42898 scFv fragment was formed by incubation of  $Gn^H/Gc$  with a 1.5 molar excess of the scFv fragment for 1 hour at 4°C. The complex was purified by SEC and eluted fractions corresponding to a monomeric and monodisperse complex were concentrated to 5 to 7 mg/ml using protein concentrator spin columns (Vivaspin) in 10 mM Tris-HCl (pH 8), 150 mM NaCl (buffer TN). The flexible linker joining  $Gn^H$  and  $Gc$  as well as the purification tag at the C-terminus of  $Gc$  were removed by adding 1 unit of biotinylated thrombin (Novagen) per mg of protein, and the mixture was

incubated at 4°C until the digestion was completed as judged by SDS-PAGE. The sample was used without further purification in crystallization trials at 18°C using the sitting-drop vapor diffusion method. Crystals grew within 5 to 10 days in the presence of 25% (w/v) polyethylenglycol (PEG) 1000, 0.1 M Hepes buffer (pH 7.5) and were flash-frozen by immersion into a cryo-protectant containing the crystallization solution supplemented with 20% (v/v) glycerol, followed by rapid transfer into liquid nitrogen.

The structure of the complex was solved by molecular replacement (MR) with Phaser from the suite PHENIX (52) using ANDV Gn<sup>H</sup>/Gc (PDB code: 6Y5 (15)) and the variable domains of an unrelated antibody (PDB code: 4UT7 (53)) as search models. The final model was built by combining real space model building in Coot (54) with reciprocal space refinement with phenix.refine to a final R(Rfree) of 21.2(24.9%). The final model, which was validated with MolProbity (55), contained aa 22 to 377 of Gn and 652 to 1086 of Gc with two disordered regions: aa 196-199 and 1064-1075. Molecular graphic images were generated using PyMOL (Schrödinger).

### **Structural representation of Gn/Gc sequence conservation**

To graphically represent the degree of sequence conservation of ADI-42898's epitope, 69 hantavirus Gn/Gc-encoding sequences were extracted (56) and aligned with Clustal Omega (57). The GenBank codes for the sequences used in our analysis are: JX465398, JX465397, JX465402, JX465399, JX465400, JX465401, JF784178, NC\_010708, EF641799, EF641806, HQ834696, FJ539167, EU929073, EU929074, HM015219, EF543526, JX465390, JX465391, JX465392, JX465393, JX465394, JX465395, JX465403, Y00386, AF143675, AB620029, AY675353, AB027115, GF796031, AY168577, AJ410616, GQ205412, AY961616, JQ082301, AF288298, GU592827, EF990916, L08756, GQ274938, HM756287, AB297666, AB433850, EF198413, AJ011648, EU072489, AJ011647, EU072488, Z69993, X55129, L36930, DQ177347, L39950, DQ284451, DQ285047, AB620104, AB620107, U26828, AB620101, U36801, U36802, AF030551, L33474, L37903, AF291703, AF028024, AF005728, FJ608550, AY363179, AF307323. The multiple sequence alignment was submitted to ENDscript (58) to calculate a conservation score at each amino acid position.



### **Enzyme-linked immunosorbent assay (ELISA) for Gn/Gc:antibody binding**

rVSVs or VLPs bearing ANDV or PUUV Gn/Gc were diluted in PBS (pH 7.4) and captured onto high-binding half-area 96-well plates (Corning) in pre-titrated amounts. Plates were then washed with PBS and blocked with a blocking/binding buffer [PBS containing 3% bovine serum albumin (BSA)] for 1 to 2 hours at 37°C. Blocked plates were exposed to a 3-fold dilution series of mAb or Fab fragment starting at 30 nM diluted in blocking/binding buffer for 1 hour at 37°C. Plates were washed with PBS and mAb binding was detected with anti-human IgG conjugated to horseradish peroxidase (HRP, Thermo Fisher) for 1 hour at 37°C. Fab fragment binding was detected with a biotin-conjugated CaptureSelect anti-human IgG-CH1 nanobody (Thermo Fisher) followed by an incubation with Streptavidin-HRP (Pierce, Cat# 21130). Plates were washed, then 1-Step Ultra TMB-ELISA Substrate Solution (Thermo Fisher) was added and quenched with 0.5 M H<sub>2</sub>SO<sub>4</sub>. Absorbance was read at 450 nm on a Cytation 5 cell imaging multi-mode reader (BioTek Instruments). Binding data were subjected to nonlinear regression analysis to derive half-maximal effective concentration (EC<sub>50</sub>) values using a variable slope sigmoidal dose-response equation (GraphPad Prism).

To measure the impact of acidic pH on Gn/Gc:mAb binding, VLPs were captured on 96-well plates and blocked as indicated above. When indicated, VLPs were exposed to a wash with PBS (pH 5.5) for 10 minutes at 37°C. After an incubation with a 3-fold dilution series of ADI-42898 at pH 7 for 1 hour at 37°C, plates were washed with PBS, and VLPs (when indicated) were exposed to a wash with PBS (pH 5.5) for 10 minutes at 37°C. The following steps were all performed at neutral pH and as described above.

### **Biolayer interferometry (BLI) assays**

To determine binding properties of IgGs and Fabs to ANDV or PUUV Gn<sup>H</sup>/Gc the Octet Red system (FortéBio) was used. To measure the binding kinetics of Gn<sup>H</sup>/Gc:mAb complexes (Fig. 1E), IgGs were captured on anti-human Fc biosensors (Sartorius, Cat# 18-5060) by dipping them into a mAb solution (10 µg/ml mAb in PBS) for 300 seconds followed by a quenching step (0.2 mg/ml BSA in PBS) for 150 seconds. IgG-loaded biosensors were exposed to PUUV or ANDV Gn<sup>H</sup>/Gc (400 nM in buffer containing 100 mM Tris-HCl, 50 mM MES, and 50 mM sodium acetate adjusted to pH 8.0, 7.5, 7.0, 6.5, 6.0, 5.5 or 5.0) for 500

seconds; the values for the last 50 seconds of the association phase were averaged and plotted using GraphPad Prism. To determine off-rates of Gn<sup>H</sup>/Gc from Gn<sup>H</sup>/Gc:mAb complexes formed on the biosensor tip surface (Fig. 2F and 3C), mAbs were immobilized on anti-human Fc biosensors and quenched as above. Next, biosensors were dipped into a Gn<sup>H</sup>/Gc solution [100 nM diluted in PBS supplemented with BSA (0.2 mg/ml)] for 200 seconds to monitor formation of the Gn<sup>H</sup>/Gc:mAb complex. Dissociation of the complex was monitored by moving the sensors into a pH-adjusted buffer (20 mM MES, 150 mM NaCl, 0.2 mg/ml BSA at pH 7.0 or 5.5) for 400 seconds. To account for potential nonspecific interactions, we dipped a sensor lacking mAb into Gn<sup>H</sup>/Gc solutions and to account for dissociation of the mAb from the sensor over the course of the experiment, we dipped the functionalized sensor into buffer lacking analyte followed by double subtractions of the signals using the Octet Red Analysis Studio software. BLI data were subjected to dissociation kinetic analysis to derive mAb dissociation rates at pH 5.5 (setting the non-specific binding term at infinite time to 0; GraphPad Prism). To derive association and dissociation rates at pH 7.0, BLI data were subjected to association-then-dissociation kinetic analysis (setting the non-specific binding term at infinite time to 0; GraphPad Prism).

To determine the apparent binding affinity ( $K_D^{app}$ ) of PUUV Gn<sup>H</sup>/Gc and ANDV Gn<sup>H</sup>/Gc to ADI-42898 (fig. S10), the mAb was captured on anti-human Fc biosensors (Sartorius, Cat# 18-5060) by dipping into a mAb solution (10 µg/ml mAb in PBS) for 300 seconds followed by a quenching step [0.2 mg/ml BSA in PBS] for 150 seconds. IgG-loaded biosensors were dipped into Gn<sup>H</sup>/Gc solutions (200 nM to 25 nM) for 300 seconds followed by a dissociation step. Experimental curves were fitted using a 1:1 binding model using GraphPad Prism. To measure Fab fragment binding affinities (fig. S10 and S12), streptavidin capture biosensors (Sartorius, Cat# 18-5019) were used to immobilize biotinylated ANDV or PUUV Gn<sup>H</sup>/Gc (100 nM) followed by a quenching step [incubation with PBS supplemented with 0.1% (w/v) BSA]. The antigen-loaded biosensors were exposed to the Fabs at 100 nM for PUUV Gn<sup>H</sup>/Gc and 500 nM for ANDV Gn<sup>H</sup>/Gc. Dissociation of Fabs from the biosensor surface was determined by transferring them into PBS supplemented with BSA. For binding responses >0.1 nm, experimental data were aligned, inter-step

corrected (to the association step) (colored traces), and fitted to a 1:1 binding model (gray traces) using the FortéBio Data Analysis Software, version 11.1 or Scrubber, version 2.0c (BioLogic Software).

### **Competition ELISA**

Competition assays monitoring the capacity of ANDV Gn/Gc-specific mAbs or soluble EC1-2 protein (sEC1-2) to inhibit rVSV:PCDH1 binding were performed as previously described (9, 20). In brief, high-binding 96-well ELISA plates (Corning, Cat# 3690) were coated with purified sEC1-2 protein (100 ng per well) overnight at 4°C and blocked with blocking buffer (5% nonfat dry milk in PBS). The membranes of rVSV-ANDV-Gn/Gc particles were labeled with a short-chain phospholipid probe, functional-component spacer diacyl lipid conjugated to biotin (FSL-biotin; Sigma-Aldrich Cat# F9182), as described (41). Biotinylated rVSV particles were incubated with the indicated dilutions of mAb, or sEC1-2 protein as a control in PBS for 1 hour at room temperature before their addition to sEC1-2-coated plates. Bound rVSV was detected by incubation with a streptavidin-HRP conjugate diluted in binding buffer (PBS supplemented with 3% BSA). Plates were washed, then 1-Step Ultra TMB-ELISA Substrate Solution (Thermo Fisher) was added and quenched with 0.5 M H<sub>2</sub>SO<sub>4</sub>. Absorbance was read at 450 nm on a Cytation 5 cell imaging multi-mode reader (BioTek Instruments).

### **Mass spectrometry (MS) of glycopeptides**

Purified VLPs bearing ANDV Gn/Gc and Gn/Gc<sup>A96T</sup> respectively were prepared for mass spectrometry as described earlier (59). In short, particles were lysed and reduced for 1 hour by incubation with a 50 mM triethylammonium bicarbonate buffer (Sigma, Cat# A6141) supplemented with 5% sodium dodecyl sulfate (SDS) (Bio-Rad, Cat# 1610301) and 5 mM dithiothreitol (Sigma, Cat# I1149). Reduced proteins were alkylated with 20 mM iodoacetamide in the dark for 30 minutes, and further denatured by incubation with aqueous phosphoric acid (1.2%; Fisher, Cat# A260-500) and loading buffer [10 mM ammonium bicarbonate buffer containing 90% methanol (Fisher, Cat# A452-1), pH 8.0]. Denatured proteins were loaded into a S-Trap micro column (Protifi, Cat# C02-micro-40) and the column was washed twice with

150  $\mu$ L loading buffer. Next, 1  $\mu$ g of sequencing grade trypsin (Promega, Cat# V511A) diluted in 50 mM ammonium bicarbonate buffer (pH 8.0) was added to the samples and incubated overnight at room temperature. After incubation, digested peptides were eluted twice with 40  $\mu$ L of a buffer containing 0.1% trifluoroacetic acid (TFA; Thermo Fisher, Cat# 28904), followed by elution with 40  $\mu$ L of a buffer containing 60% acetonitrile (Fisher, Cat# A955-4) and 0.1% TFA, and then dried in a vacuum centrifuge. Samples were resuspended in an ammonium bicarbonate buffer (50 mM, pH 8.0) supplemented with 1  $\mu$ g of sequencing grade chymotrypsin (Promega, Cat# V1061) and digested at room temperature for 5 h. In addition, the ANDV Gn/Gc<sup>A96T</sup> protein sample was treated with the endoglycosidase PNGase F (New England Biolabs, Cat# P0705S) to enzymatically remove N-linked oligosaccharides, which is accompanied by the deamidation of asparagine residues and provides an indirect indication of N-glycosylation sites.

To prepare for mass spectrometry analysis, the samples were desalted using a 96-well plate filter (Orochem) packed with 1 mg of Oasis HLB C-18 resin (Waters). Briefly, samples were resuspended in 100  $\mu$ L of a buffer containing 0.1% TFA and loaded onto the HLB resin, which was previously equilibrated with 100  $\mu$ L of the same buffer. After washing with 100  $\mu$ L of 0.1% TFA, the samples were eluted with a buffer containing 70  $\mu$ L of 60% acetonitrile and 0.1% TFA, and then dried in a vacuum centrifuge. Samples were resuspended in 8  $\mu$ L of 0.1% TFA and loaded onto a Dionex RSLC Ultimate 300 (Thermo Scientific), and coupled online with an Orbitrap Fusion Lumos (Thermo Scientific). Peptides were separated using a 195 minute linear gradient consisting of 0-32% acetonitrile in 0.1% formic acid over 180 minutes followed by 5 minutes of 32-80% acetonitrile and 5 minutes of 80% acetonitrile in 0.1% formic acid at a flow rate of 300 nl/minute. The mass spectrometer was set to acquire spectra in a data-dependent acquisition (DDA) mode. Briefly, the full MS scan was set to 400 to 2000 m/z in the orbitrap with a resolution of 120,000 (at 200 m/z) and an AGC target of  $4 \times 10^5$ . MS/MS was performed in the orbitrap with a resolution of 7500 using an automatic gain control (AGC) target of  $5 \times 10^4$  and a normalized collision energy (NCE) of 30 for fragmentation of glycopeptide ions. Protein Metrics software (Version 4.6) was used to search the post-translational modifications from raw files.

### **Virus attachment assay**

rVSV-ANDV-Gn/Gc particles were incubated with mAb (300 nM) or serum from rVSV-ANDV-Gn/Gc-infected Syrian hamsters (a generous gift of D. Safronetz, Public Health Agency of Canada) at room temperature for 1 hour. These rVSV:mAb complexes were spin-oculated onto pre-chilled HUVECs at 1,000 rpm and 4°C for 10 minutes followed by an incubation on a cooling plate at 6°C for 30 minutes. Unbound virus was removed by washing with cold PBS. Cells were harvested in PBS, RNA was isolated using PureLink RNA Mini Kit (Invitrogen, Cat# 12183018A) according to manufacturer's protocols, and cell-bound virus was quantified by quantitative reverse transcription PCR (RT-qPCR) detecting the open-reading frame encoding the VSV matrix protein (M). For the one-step RT-qPCR, the isolated RNA was mixed with VSV M-specific probe (IDT, 10 pmol, 56-FAM/TGTGGCAGC/ZEN/CGCTGTATCCCATT/3IABkFQ), forward primer (IDT, 25 pmol, 5'-AATCGTCCGTTTCAGAACATAC), reverse primer (IDT, 25 pmol, 5'-GAAGAACCCTAAAAAGCCAAG) and TaqPath 1-Step RT-qPCR Master Mix (Life Technologies, Cat# A15299). All samples were run and analyzed using the QuantStudio 3 Real-Time PCR System device (Applied Biosystem). Serial ten-fold dilutions of a plasmid encoding the full-length genomic cDNA of rVSV-ANDV-Gn/Gc were used to generate a standard curve for quantification.

### **Virus elution assay**

rVSV-ANDV-Gn/Gc particles were incubated with ADI-42898 (100 nM) or without mAb at room temperature for 1 hour. These rVSV:mAb complexes were spin-oculated onto pre-chilled HUVECs at 2,500 rpm and 4°C for 45 minutes. Cells were moved onto a cooling plate and washed three times with cold PBS. After every wash step, cells were harvested in PBS, RNA was isolated using the PureLink RNA Mini Kit (Invitrogen, Cat# 12183018A) according to manufacturer's protocols and cell-bound virus was quantified by RT-qPCR detecting the open-reading frame encoding the VSV M protein as described in the "Virus attachment assay" section.

### **Fusion-infection assay**

To evaluate the ability of mAbs to inhibit fusion, rVSV particles bearing ANDV or PUUV Gn/Gc were pre-incubated with increasing amounts of mAb (as indicated) for 1 hour at 4°C. rVSV:mAb complexes were bound to pre-chilled HUVECs by centrifugation at 2,500 rpm and 4°C for 1 hour. Cells were placed on ice and unbound virus washed away with cold PBS. Membrane fusion was initiated by incubating HUVECs at 37°C for 1 minute in DMEM-F12 media adjusted to pH 5.5, followed by shifting cells back to 4°C. Further rounds of infection were prevented by the exchange of media supplemented with 20 mM NH<sub>4</sub>Cl, and infected cells were maintained at 37°C for 14 hours post-infection before automated counting of eGFP<sup>+</sup> and mNG<sup>+</sup> cells using a Cytation 5 cell imaging multi-mode reader (BioTek Instruments) and a Cell-Insight CX5 imager (Thermo Fisher) including onboard software.

### **Generation and selection of affinity-matured ADI-42898 variants**

Affinity-matured variants of ADI-42898 carrying single-position mutations were generated by introducing mutations into each position of the complementary determining regions (CDRs) 1, 2, and 3 of the V<sub>H</sub> and V<sub>L</sub> genes of ADI-42898 by overlap extension PCR. Briefly, forward or reverse-priming oligos (IDT) encoding 'NNK' or 'MNN' degenerate codons at a single site were used to amplify overlapping fragments. The fragments were assembled into full-length V<sub>H</sub> or V<sub>L</sub> regions by a second nested PCR with flanking primers which contained 40 base pairs of 5' and 3' homology to linearized yeast expression vectors to allow insertion by homologous recombination. The resulting 76 single-position libraries were then transformed into *Saccharomyces cerevisiae* following the lithium acetate method for chemical transformation (60). Individual colonies from single-position libraries were validated by Sanger sequencing and about 13 individual yeast colonies from each single-position library were picked for production of 1,020 Fab fragments of ADI-42898 sequence variants.

Eight Fab variants carrying single-point mutations displayed improved ANDV Gn<sup>H</sup>/Gc binding affinities. These beneficial mutations were combined to generate 47 combinatorial mutation variants which were

produced as full-length IgGs in *Saccharomyces cerevisiae* following established protocols (50). Resulting ADI-42898 variants were screened for further improvements in binding activity by BLI assays (FortéBio).

### **Polyreactivity assay**

Antibody polyreactivity was measured as described previously (26). Briefly, soluble membrane protein and soluble cytosolic protein fractions obtained from CHO cells were biotinylated using NHS-LC-Biotin reagent (Thermo Fisher). Yeast cells presenting IgGs on their surface were incubated with biotinylated CHO cell preparations on ice, followed by two washes with ice-cold PBS containing 0.1% w/v BSA and incubated with a secondary labeling mix containing ExtrAvidin-R-PE (Sigma-Aldrich, Cat# E4011), anti-human LC-fluorescein isothiocyanate (FITC) (Southern Biotech, Cat# 2062-02), and propidium iodide (Invitrogen) for 15 minutes. Cells were washed with PBS containing 0.1% w/v BSA, resuspended, and analyzed by flow cytometry on a FACS Canto II (BD Biosciences). The mean fluorescence intensity of binding was normalized using control antibodies that display low, medium, or high polyreactivity to assess the non-specific binding.

### **Bank vole challenge studies**

The neutralizing potential of human mAbs against PUUV/Suo challenge in vivo was investigated in an established experimental PUUV reservoir host model system (40). Bank vole (*Myodes glareolus*) animal protocols were approved by the Animal Experimental Board of Finland (license numbers ESAVI/28410/2019 and ESAVI/45015/2021). Laboratory-bred adult bank voles were housed under Biosafety level 3 conditions in an IsoCage biocontainment system (Scanbur) in groups of 4 to 5 animals and provided standard rodent pellets and water ad libitum. Both sexes of a 50:50 distribution were used in experimental groups when possible; randomization and blinding were not performed. Adult bank voles were challenged with 500 focus-forming units (FFU) of PUUV/Suo by subcutaneous inoculation. In a prophylactic treatment regimen, bank voles were intraperitoneally (i.p.) injected with mAbs (about 5 mg/kg) (or PBS as vehicle control) 4 hours before challenge. The animals were euthanized 72 hours after

virus inoculation by cervical dislocation, after which RNA was isolated from lungs and spleen using TRIzol Reagent (Thermo Fisher, Cat# 15596026) according to the manufacturer's instructions. Virus RNA loads were assessed by PUUV S segment RT-qPCR as described previously (61) and the results were normalized to the total RNA concentration of the samples and presented as S segment copy number per  $\mu\text{g}$  of total RNA. Viral RNA load in animal tissue was analyzed using a Kruskal-Wallis test with Dunn's correction for multiple comparisons (GraphPad Prism). All bank voles from two independent experiments were included in the data analysis; no outliers were excluded.

### **Syrian hamster challenge studies**

Syrian golden hamsters (Envigo, Cat# HsdHan AURA 089), 100 to 120 grams, were exposed intramuscularly to 200 PFU of ANDV strain Chile-9717869 diluted in 0.1 ml of PBS. On day 3, 6 or 7 post-exposure, hamsters were treated i.p. with indicated amounts (25, 2, or 0.5 mg/kg) of mAb diluted in 0.8 ml of PBS. Blood samples (0.25 ml) were collected by venipuncture of the anterior vena cava on day 7 or 8 post-challenge (Fig. 5C) to assess human IgG concentrations in serum. Hamsters were monitored daily for clinical signs of disease, morbidity, and mortality for 28 days. Moribund animals, defined as those experiencing severe respiratory distress or showing unresponsiveness, were humanely euthanized according to IACUC-approved criteria. Human IgG concentrations in hamster serum collected at day 7 or 8 post-exposure (Fig. 5C) were determined by quantitative capture ELISA in order to exclude any hamsters that remained human IgG-negative following antibody treatment, a phenomenon that has been described previously (62). Hamsters that were human IgG negative at day 7 or 8 were deemed untreated and removed from the dataset.

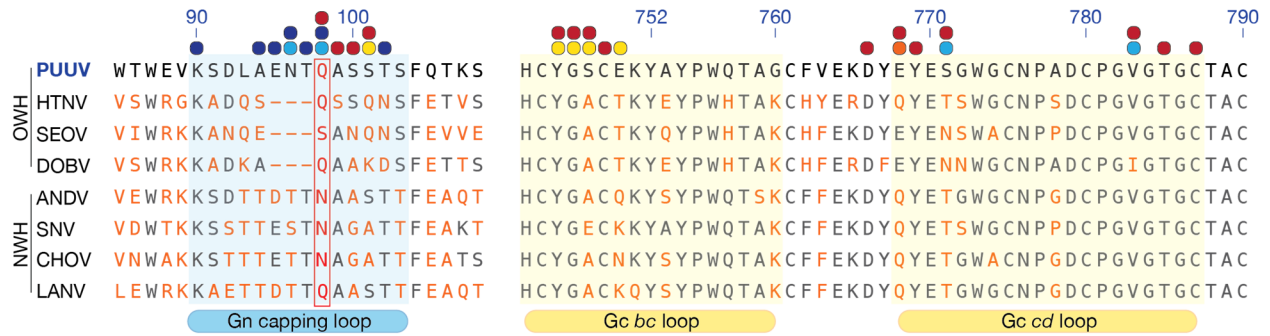
In longitudinal ANDV challenge studies, Syrian golden hamsters were exposed intramuscularly to 200 PFU of ANDV strain Chile-9717869 diluted in 0.2 ml of PBS. On day 2, 4, 5, 6, 7, 8, 9, 10, 11, and 12 post virus exposure, three animals were euthanized by exsanguination through cardiac puncture. Lung tissues were collected by necropsy, homogenized and lung virus loads were determined by plaque assay. Serum virus



titers were also assessed by plaque assay. All hamsters from one experiment were included in the data analysis; no outliers were excluded.

### **Human IgG ELISA from hamster serum**

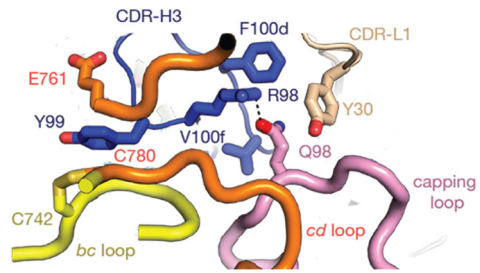
ELISA plates were coated with sheep anti-human IgG capture antibody at 0.1  $\mu\text{g}$  per well over night at 4°C. Coated plates were washed with PBS/0.1% Tween 20 and blocked with Casein buffer (G-Biosciences) for 2 hours at room temperature. A standard curve for ADI-42898 was generated by 2-fold dilutions from 500 ng/ml to 15.6 ng/ml of mAb in assay buffer (Casein buffer/10% normal hamster serum). Standards and diluted day 7 or 8 hamster serum samples were added to coated wells and incubated at 37°C for 1 hour. Antibodies were detected by adding goat anti-human IgG-HRP conjugate for 1 hour at 37°C. Absorbance values were measured using a SpectraMax 5 plate reader (Molecular Devices) and standard curves were generated using nonlinear regression analysis (four-parameter, variable slope sigmoidal dose-response equation; GraphPad Prism). Absorbance values from samples with unknown human antibody concentrations were applied to the standard curve to determine the concentration of human IgG. Hamsters that were human IgG negative at day 7 or 8 (Fig. 5C) were deemed untreated and removed from the dataset.



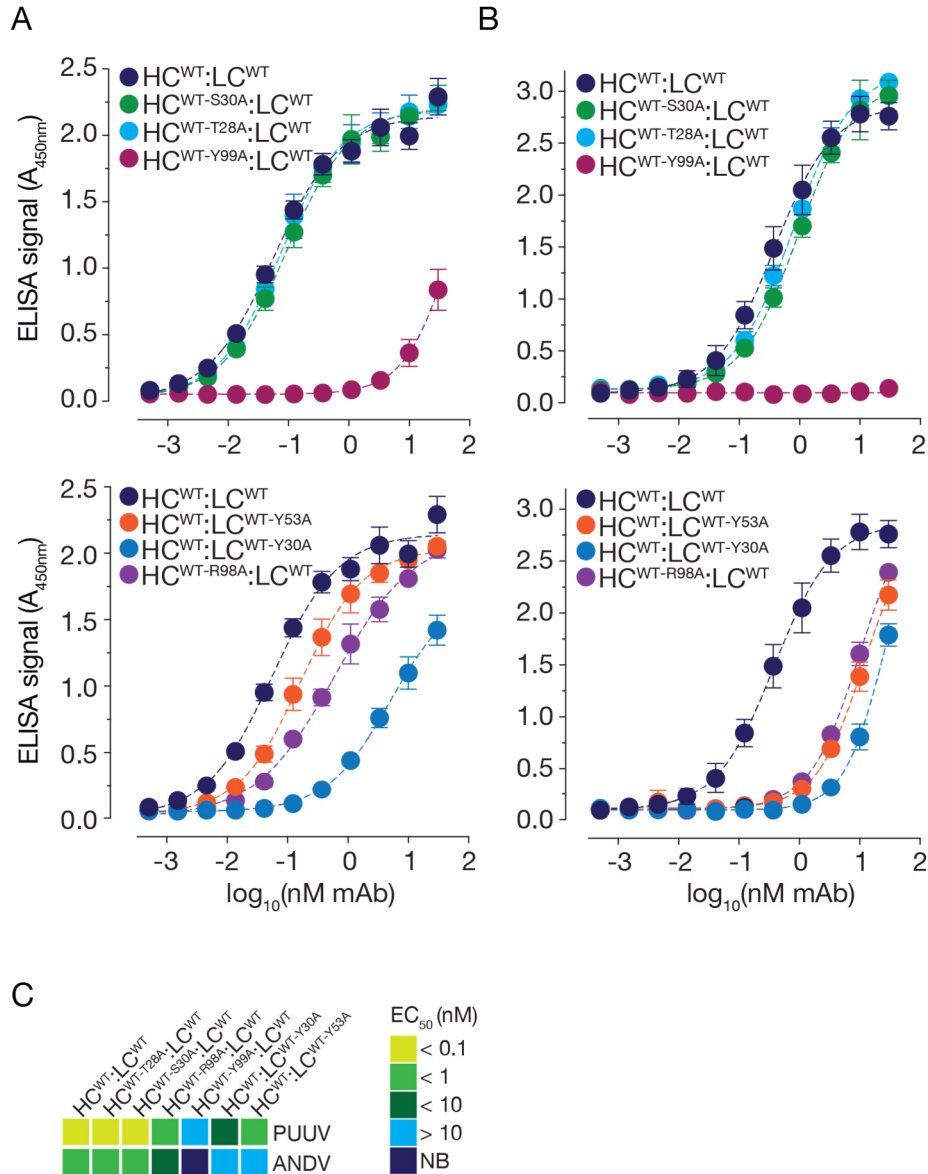
ADI-42898 paratope contact site

- CDR-L1
- CDR-L2
- CDR-H1
- CDR-H2
- CDR-H3

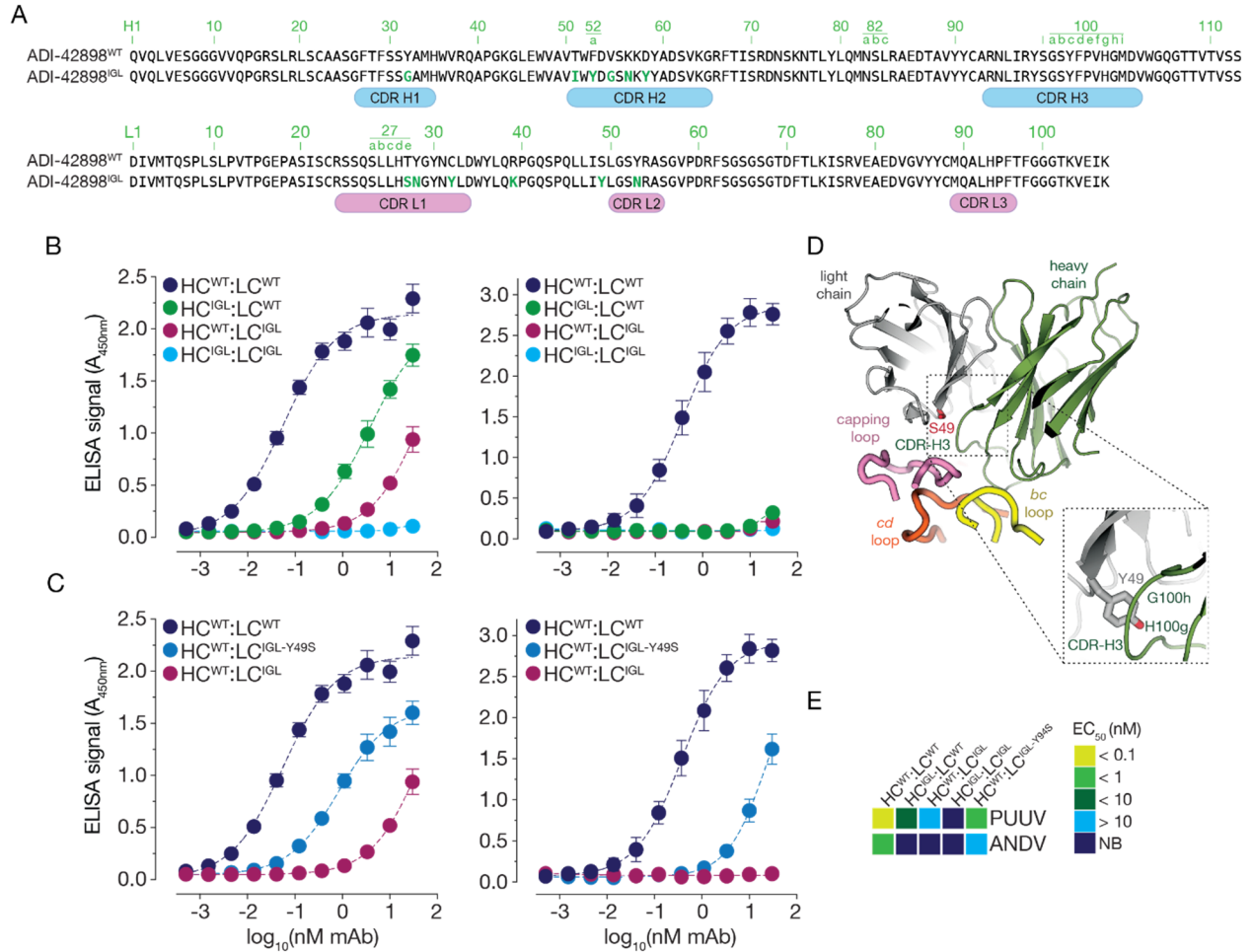
**Fig. S1. Epitope of ADI-42898 in hantaviral Gn/Gc.** Annotated amino acid sequence alignment of Old World hantavirus (OWH) and New World hantavirus (NWH) Gn/Gc (PUUV [strain Astrup], GenBank AJC50718; HTNV [strain 76-118], GenBank Y00386.1; SEOV [strain SR-11], GenBank M34882.1; DOBV [strain Ano-Poroia/Af19], GenBank NP\_942554.1; ANDV [strain Chile-9717869], GenBank MT956623.1; SNV [strain NM H10], GenBank KT885045.1; CHOV [strain 588] GenBank KT983772.1; LANV [strain 510B], GenBank AF005728.1) (PUUV Gn/Gc numbering). Gray, conserved residues; orange, divergent residues. Position of PUUV<sup>Q98</sup> and equivalent residues in divergent OWH and NWH Gn/Gc proteins are boxed and labeled in red. ADI-42898 paratope contact sites (distance <5 Å, determined with PyMol) are indicated and colored according to contact complementarity-determining regions (CDRs).



**Fig. S2. ADI-42898:Gn<sup>H</sup>/Gc interface formation.** Amino acid residues participating in binding interface (enlarged view from Fig. 1C). ADI-42898 residues are numbered according to the Kabat scheme. CDR-H, CDR-L: complementarity-determining regions of the heavy chain and light chains, respectively.

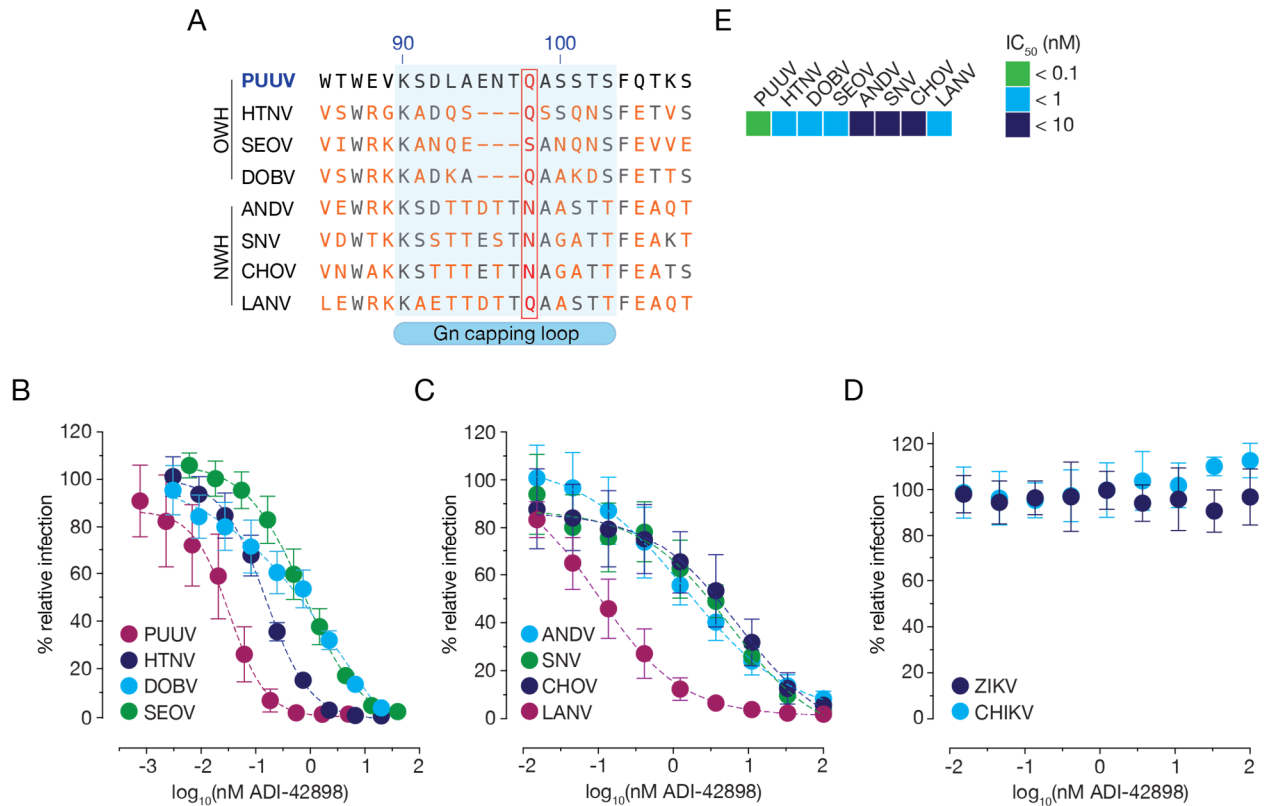


**Fig. S3. Characterization of the ADI-42898 paratope.** (A and B) Capacity of mAbs carrying alanine substitutions in Gn/Gc contact sites (identified in Fig. 1B and C) to bind rVSV-PUUV-Gn/Gc (A) or rVSV-ANDV-Gn/Gc (B) was measured by ELISA. Data are presented as averages  $\pm$  SD,  $n = 4$  to 6 from two to three independent experiments. (C) Heatmap of EC<sub>50</sub> values isolated from PUUV and ANDV Gn/Gc dose-response binding curves (A and B) derived by nonlinear regression analysis. Data points are colored according to the mAb's binding potency. Also see data file S2 for EC<sub>50</sub> values. mAbs with EC<sub>50</sub> values of >100 nM were designated as non-binding mAbs (NB). WT, wild type.

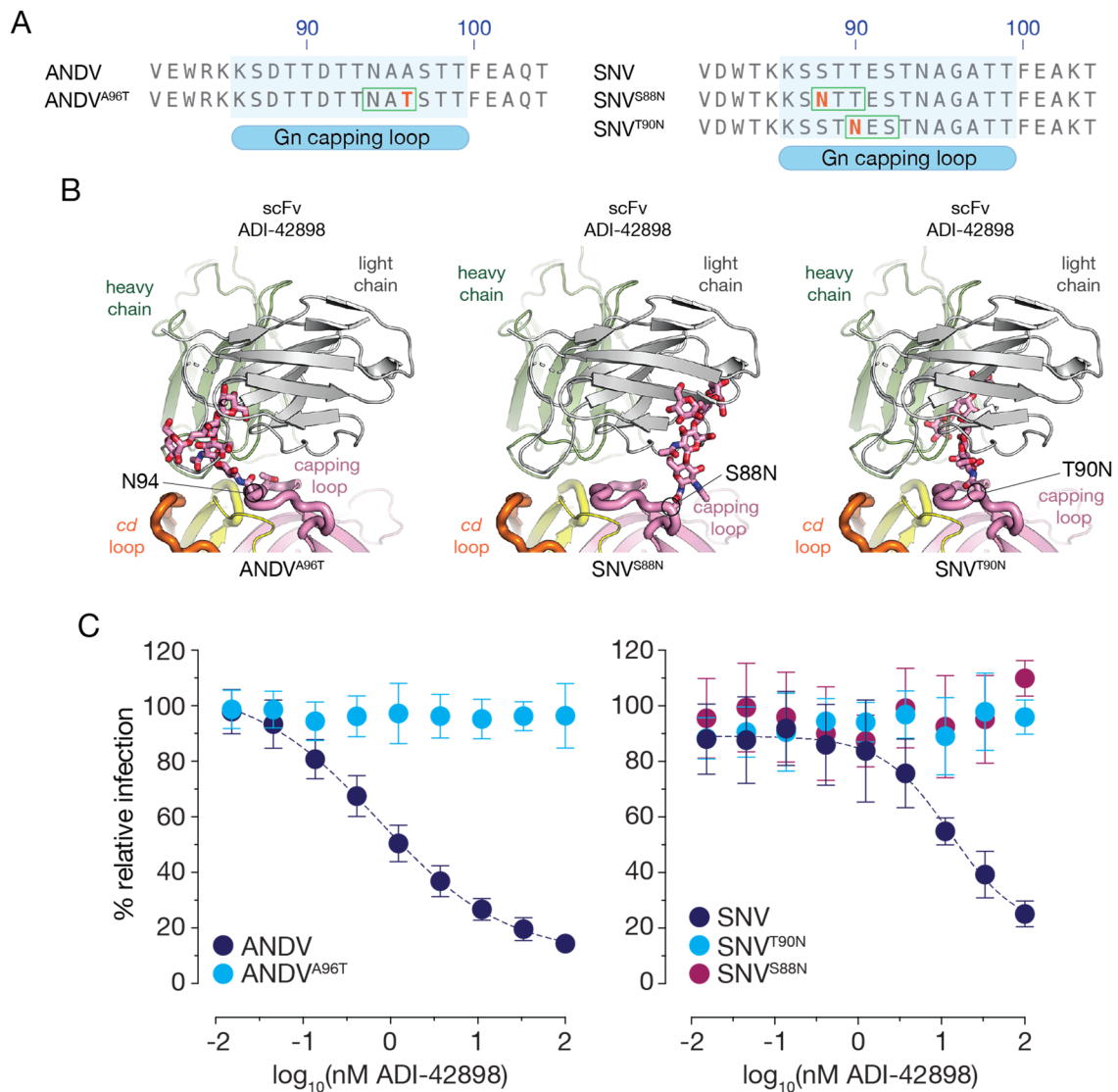


**Fig. S4. Germline origin of ADI-42898 and sequence determinants of its binding activity. (A)** Alignment of mature heavy chain variable region ( $V_H$ ) and light chain variable region ( $V_L$ ) sequences (ADI-42898<sup>WT</sup>) with the reconstruction of an inferred germline (IGL) ancestor (ADI-42898<sup>IGL</sup>) bearing the closest human germline V and J gene segments and mature CDR-H3 (Kabat numbering). Antibody sequences were analyzed using Abysis (<http://www.bioinf.org.uk/software>) and IMGT (<http://www.imgt.org>) databases. Amino acid insertions into longer loops are indicated by lowercase letters (labeled green). Amino acid residues divergent from the IGL sequence are labeled in green. **(B)** Capacity of mAb variants carrying IGL ancestor sequences to bind rVSV-PUUV-Gn/Gc (left panels) or rVSV-ANDV-Gn/Gc (right panels) was measured by ELISA. Data are presented as averages  $\pm$  SD,  $n = 4$  from two independent experiments. **(C)** Capacity of mAb variants carrying IGL ancestor sequences (and a Y49S somatic hypermutation) to bind rVSV-PUUV-Gn/Gc (left panels) or rVSV-ANDV-Gn/Gc (right panels) was measured by ELISA. Data are

presented as averages  $\pm$  SD,  $n = 4$  from two independent experiments. **(D)** Ribbon representation of ADI-42898:PUUV Gn<sup>H</sup>/Gc contact surface with three discontinuous loops (Gn capping loop, Gc *bc* loop, and Gc *cd* loop) engaging the mAb's HC and LC. Somatic hypermutation Y49S located in FR2 of the LC is highlighted (also see fig. S4A). The spatial organization of the CDR-H3 proximal to Y49 in ADI-42898<sup>IGL</sup> was enlarged for clarity (dashed rectangle). **(E)** Heatmap of EC<sub>50</sub> values isolated from PUUV and ANDV Gn/Gc dose-response binding curves (B and C) derived by nonlinear regression analysis. Data points are colored according to the mAb's binding potency. Also see data file S2 for EC<sub>50</sub> values. mAbs with EC<sub>50</sub> values of >100 nM were designated as non-binding mAbs (NB).



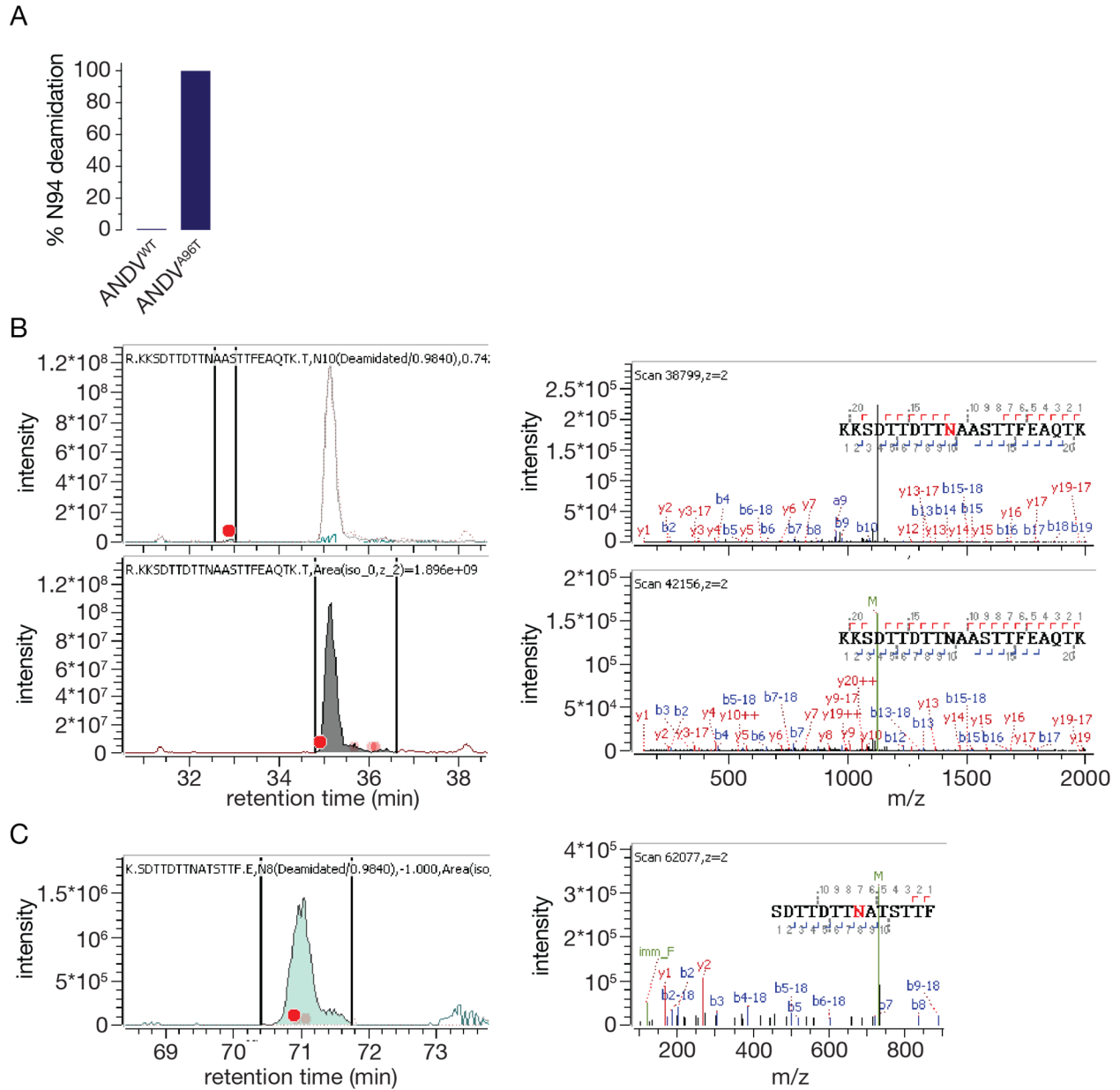
**Fig. S5. ADI-42898 neutralization determinants.** (A) Amino acid sequence alignment of OWH and NWH Gn/Gc capping loops (PUUV [strain Astrup], GenBank AJC50718; HTNV [strain 76-118], GenBank Y00386.1; SEOV [strain SR-11], GenBank M34882.1; DOBV [strain Ano-Poroia/Af19], GenBank NP\_942554.1; ANDV [strain Chile-9717869], GenBank MT956623.1; SNV [strain NM H10], GenBank KT885045.1; CHOV [strain 588] GenBank KT983772.1; LANV [strain 510B], GenBank AF005728.1) (PUUV Gn/Gc numbering). Gray, conserved residues; orange, divergent residues. Position of PUUV<sup>Q98</sup> and equivalent residues in divergent Gn/Gc complexes are boxed and labeled in red. (B and C) ADI-42898 neutralization profiles of rVSVs bearing OWH (B) or NWH (C) Gn/Gc. Data are presented as averages  $\pm$  SD,  $n = 8$  to 12 from three to four independent experiments. (D) ADI-42898 neutralization profiles of rVSV bearing the CHIKV surface protein and ZIKV strain MR766. Data are presented as averages  $\pm$  SD,  $n = 4$  to 9 from two to three independent experiments. (E) Heatmap of IC<sub>50</sub> values isolated from rVSV dose-response neutralization curves (B and C) derived by nonlinear regression analysis. Data points are colored according to ADI-42898's neutralization potency. Also see data file S2 for IC<sub>50</sub> values.



**Fig. S6. Characterization of rVSV-ANDV-Gn/Gc and rVSV-SNV-Gn/Gc mutants resistant to ADI-42898 neutralization.** (A) Amino acid sequence alignment of Gn of ANDV and ANDV<sup>A96T</sup> (left with ANDV Gn/Gc numbering) as well as SNV, SNV<sup>S88N</sup> and SNV<sup>T90N</sup> (right with SNV Gn/Gc numbering). Orange, viral neutralization escape mutations. Positions of sequons (N-X-S/T) introduced in escape variants are boxed in green. (B) Ribbon representations of X-ray structures of PUUV Gn<sup>H</sup>/Gc contact sites with an scFv fragment of ADI-42898. The core of predicted N-linked glycans (Man<sub>3</sub>GlcNAc<sub>2</sub>) attached at positions 92, 94 and 98 (PUUV Gn/Gc numbering) were modeled onto Gn<sup>H</sup>/Gc. (C) Capacity of ADI-42898 to

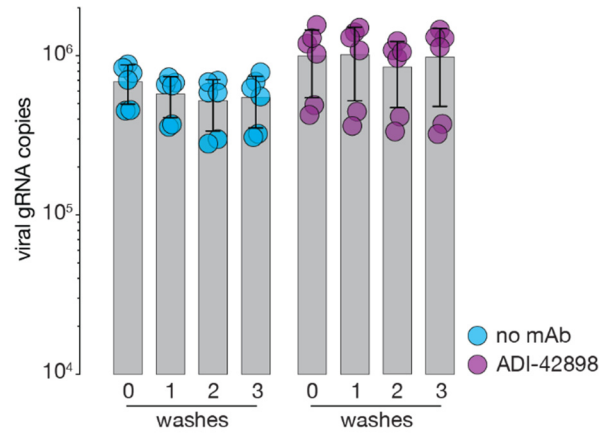


neutralize rVSV-ANDV-Gn/Gc or rVSV-SNV-Gn/Gc bearing neutralization-escape variants in their Gn capping loop. Data are presented as averages  $\pm$  SD,  $n = 4$  to 12 from two to four independent experiments.

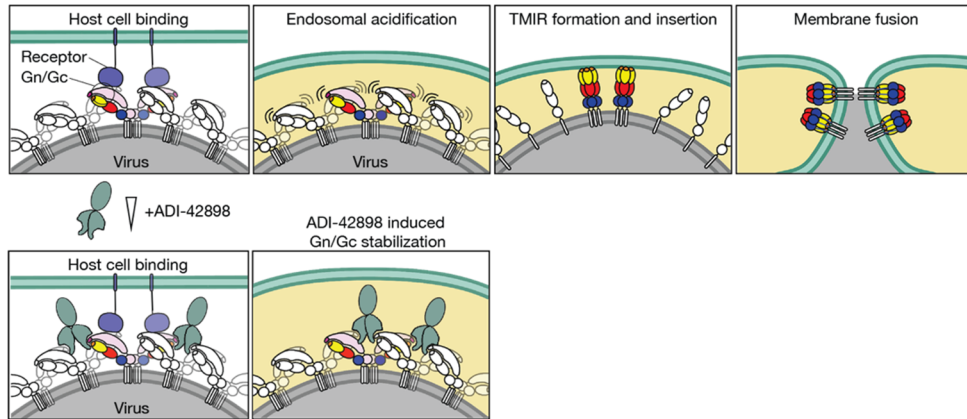


**Fig. S7. N-linked glycosylation of ANDV<sup>A96T</sup>.** (A) Occupancy of N-glycans at residue N94 in ANDV<sup>WT</sup> and ANDV<sup>A96T</sup> proteins isolated from VLPs. N-glycosylation was indicated by the residue's deamidation and determined by LC-MS/MS. (B) Extracted ion chromatograms (left panels) with residue N94 indicated as red dots and MS/MS spectra (right panels) of ANDV<sup>WT</sup> protein. Top panels show deamidated and bottom panels unmodified peptides comprising N94, confirming that ANDV<sup>WT</sup> is a non-glycosylated protein. (C) Extracted ion chromatogram (left panel) with residue N94 indicated as red dot and MS/MS spectrum (right panel) of ANDV<sup>A96T</sup> protein. Panels show deamidated peptides comprising N94. ANDV<sup>A96T</sup> protein was

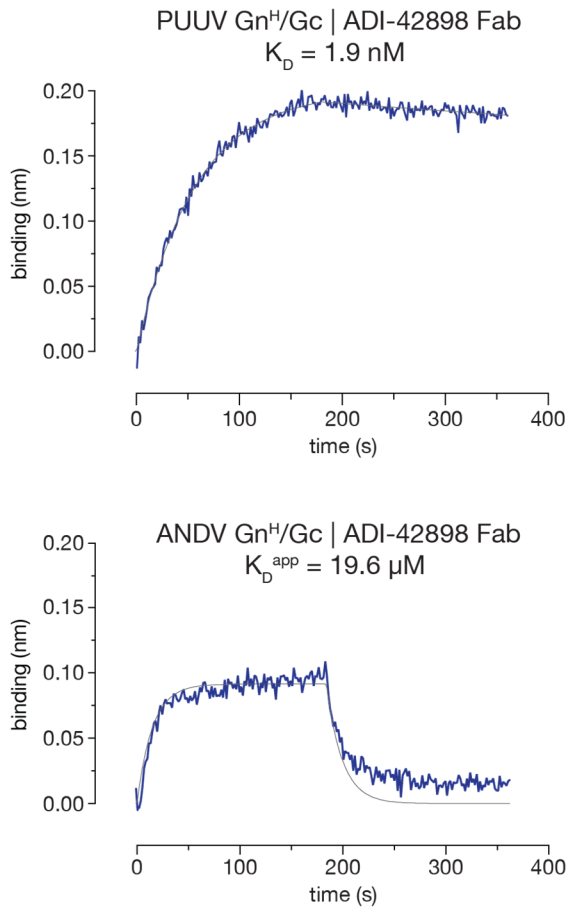
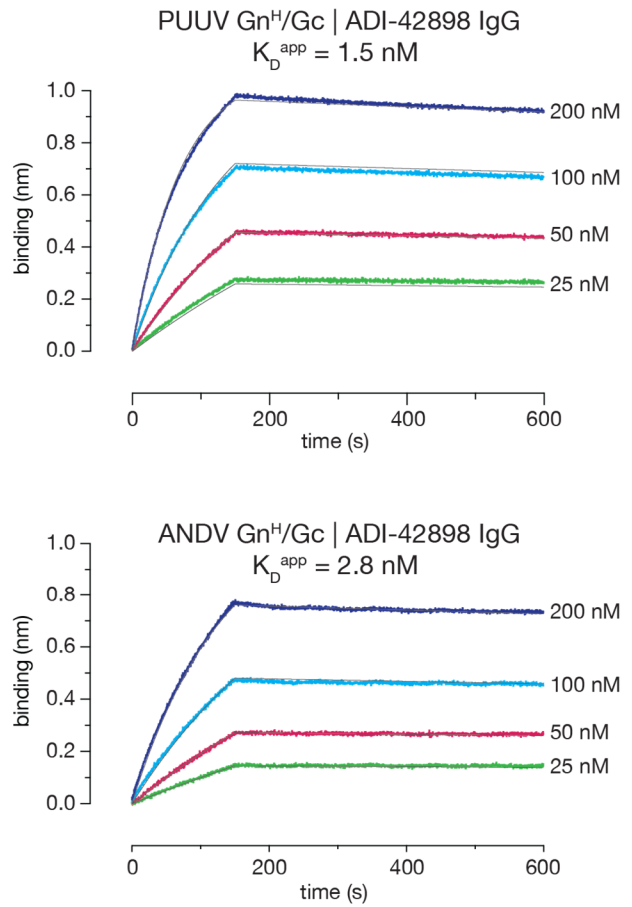
deamidated close to 100%, and no corresponding unmodified peptide was detected by MS. MS data were analyzed with Protein Metrics software.



**Fig. S8. Capacity of ADI-42898 to elute rVSV-ANDV-Gn/Gc from HUVECs.** Bound viral particles were enumerated after washing HUVECs with cold PBS by RT-qPCR detecting rVSV genomic RNA (gRNA). Data are presented as averages  $\pm$  SD,  $n = 6$  from 3 independent experiments.



**Fig. S9. Schematic mechanistic model of ADI-42898 stabilizing the Gn/Gc pre-fusion complex.** Gn, light pink; Gc domain I, red; Gc domain II, yellow; Gc domain III, blue. TMIR, target membrane-interacting region.

**A****B**

**Fig. S10. Binding properties of ADI-42898.** (A) BLI sensorgrams for ADI-42898 Fab binding to PUUV and ANDV Gn<sup>H</sup>/Gc. Biotinylated Gn<sup>H</sup>/Gc was loaded onto probes, and dipped into solutions of ADI-42898 Fab (100 nM for PUUV Gn<sup>H</sup>/Gc, 500 nM for ANDV Gn<sup>H</sup>/Gc). Experimental curves (colored traces) were fit using a 1:1 binding model (gray traces) to estimate  $K_D$ . Although data could be described accurately with a 1:1 binding model, given that ANDV Gn<sup>H</sup>/Gc is a mixture of monomers and dimers, we cannot rule out avidity effects and therefore report apparent  $K_D$  values ( $K_D^{app}$ ; apparent equilibrium constant). (B) BLI sensorgrams for ADI-42898 IgG binding to PUUV and ANDV Gn<sup>H</sup>/Gc. ADI-42898 was loaded onto probes, which were dipped in solutions of Gn<sup>H</sup>/Gc at the indicated concentrations. Experimental curves (colored traces) were fit using a 1:1 binding model (gray traces) to estimate  $K_D^{app}$ . Although data could be described accurately with a 1:1 model, given that ANDV Gn<sup>H</sup>/Gc is a mixture of monomers and dimers and

given the dimeric nature of IgGs, we cannot rule out avidity effects and therefore report  $K_D^{\text{app}}$  values.

Results from a representative experiment are shown.

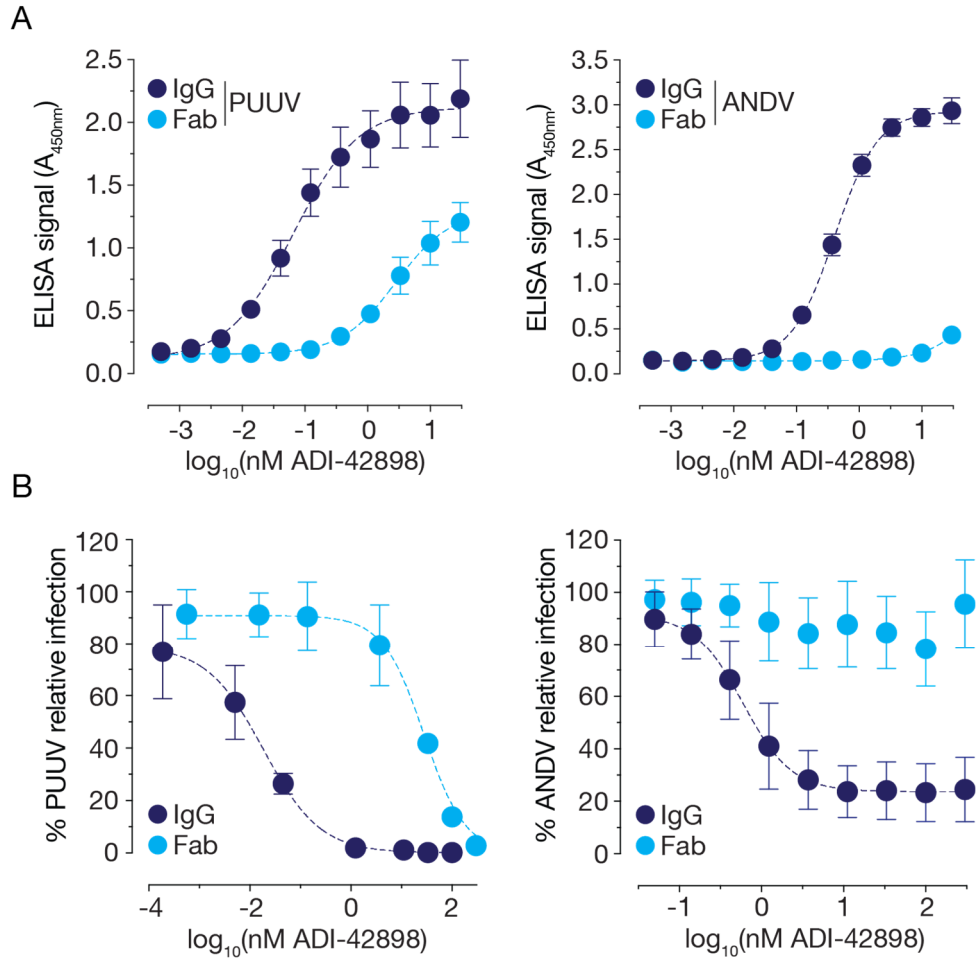


**Fig. S11. Importance of ADI-42898 valency for its binding and neutralization profiles.** (A) Capacity of IgGs and monovalent Fabs to bind ANDV and PUUV Gn/Gc-decorated VLPs as measured by ELISA. Data are presented as averages  $\pm$  SD,  $n = 6$  from three independent experiments. (B) Capacity of IgGs and monovalent Fabs to inhibit authentic PUUV (strain Kazan) and ANDV (strain Chile-9717869) infection. Data are presented as averages  $\pm$  SD,  $n = 4$  to 6 from two independent experiments.



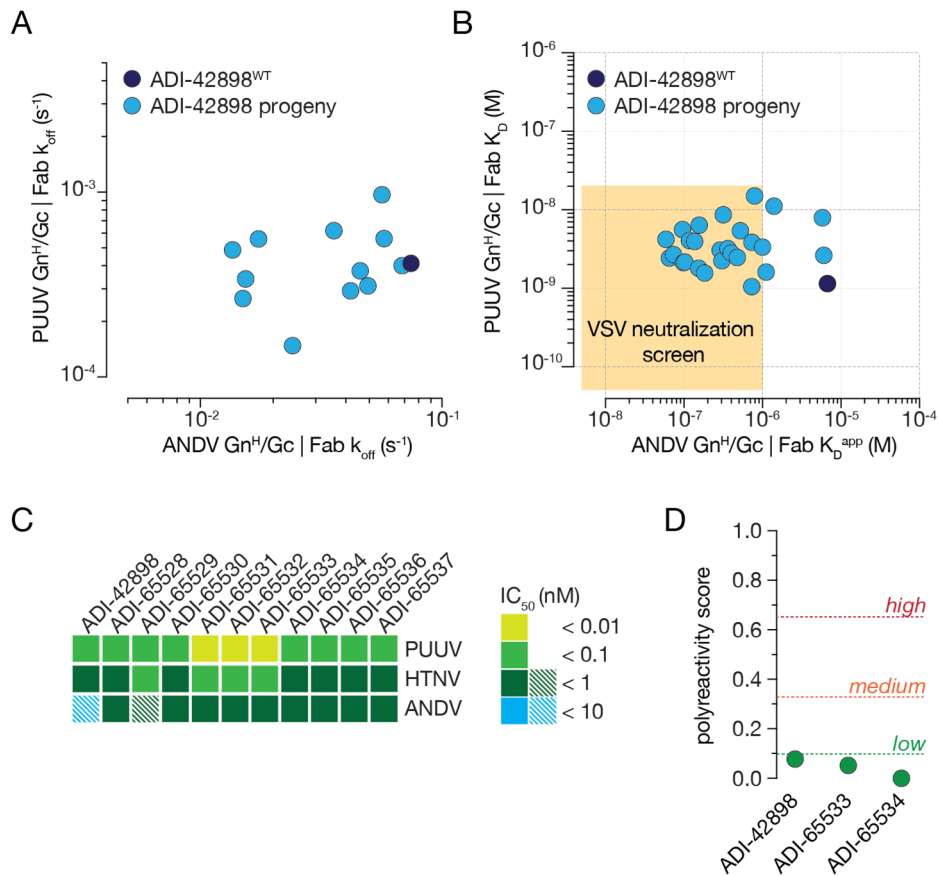


**Fig. S12. Engineering of ADI-42898 for improved affinity towards ANDV Gn/Gc.** (A) Graphical representation of dissociation rate constants ( $k_{off}$ ) of Fab fragments of ADI-42898 and 12 progeny variants bearing single-mutant CDRs bound to ANDV and PUUV Gn<sup>H</sup>/Gc, as assessed by BLI. (B) Kinetic constants of 26 Fabs carrying combinatorial mutations for binding to ANDV and PUUV Gn<sup>H</sup>/Gc are shown, as determined by BLI. Clones selected for testing against rVSV-ANDV-Gn/Gc infection are indicated by the yellow shaded area. For Fab sequences and BLI data also see data file S1. (C) Ten ADI-42898 progeny variants presenting the highest increase in neutralization potency against rVSV-ANDV-Gn/Gc were advanced for testing of their activity against divergent Gn/Gc proteins. Heatmap of  $IC_{50}$  values from rVSV-PUUV-Gn/Gc, rVSV-HTNV-Gn/Gc, and rVSV-ANDV-Gn/Gc dose-response neutralization curves derived by nonlinear regression analysis. Data points are colored according to mAb neutralization potency. Also see data file S2 for  $IC_{50}$  values. mAbs leaving an un-neutralized virus fraction are shown as striped data points on the map. An un-neutralized virus fraction is defined as a residual normalized virus infection

of >5% at the highest mAb concentration tested. Data are presented as averages,  $n = 6$  from two independent experiments are shown. **(D)** Polyreactivity scores for mAbs were determined as reported previously (26). Thresholds for high, medium, and low polyreactivity are indicated by dashed lines.

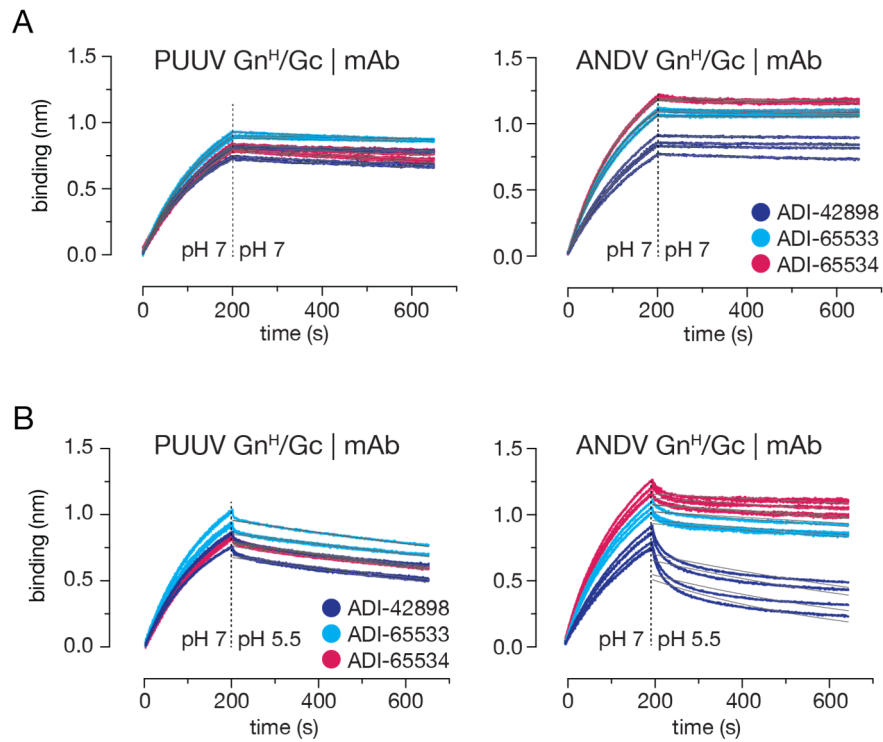


**Fig. S13. Kinetic binding studies of ADI-42898 and affinity-matured mAbs to Gn<sup>H</sup>/Gc.** (A) BLI sensorgrams showing binding kinetics of PUUV (left panel) and ANDV (right panel) Gn<sup>H</sup>/Gc to ADI-42898, ADI-65533, and ADI-65534 at pH 7.0. (B) BLI sensorgrams for association of PUUV (left panel) and ANDV (right panel) Gn<sup>H</sup>/Gc to mAbs at pH 7.0, followed by dissociation of Gn<sup>H</sup>/Gc at pH 5.5 (pH shift indicated by dotted line). Experimental curves (colored traces) were fitted using a 1:1 binding model (gray traces) using GraphPad Prism.  $n = 4$  from four independent experiments are shown.

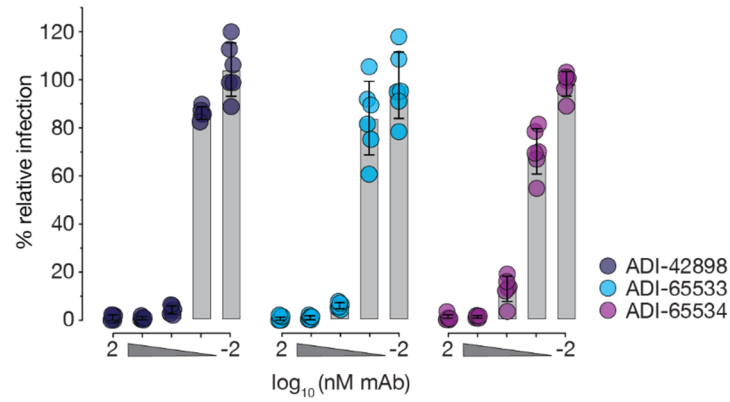


**Fig. S14. Blocking of PUUV Gn/Gc-mediated fusion-infection.** Capacity of ADI-42898, ADI-65533, and ADI-65534 to inhibit PUUV Gn/Gc-mediated fusion-infection. rVSV-PUUV-Gn/Gc particles were pre-incubated with mAb, followed by fusion-infection of HUVECs. Data are presented as averages  $\pm$  SD,  $n = 6$  from two independent experiments.

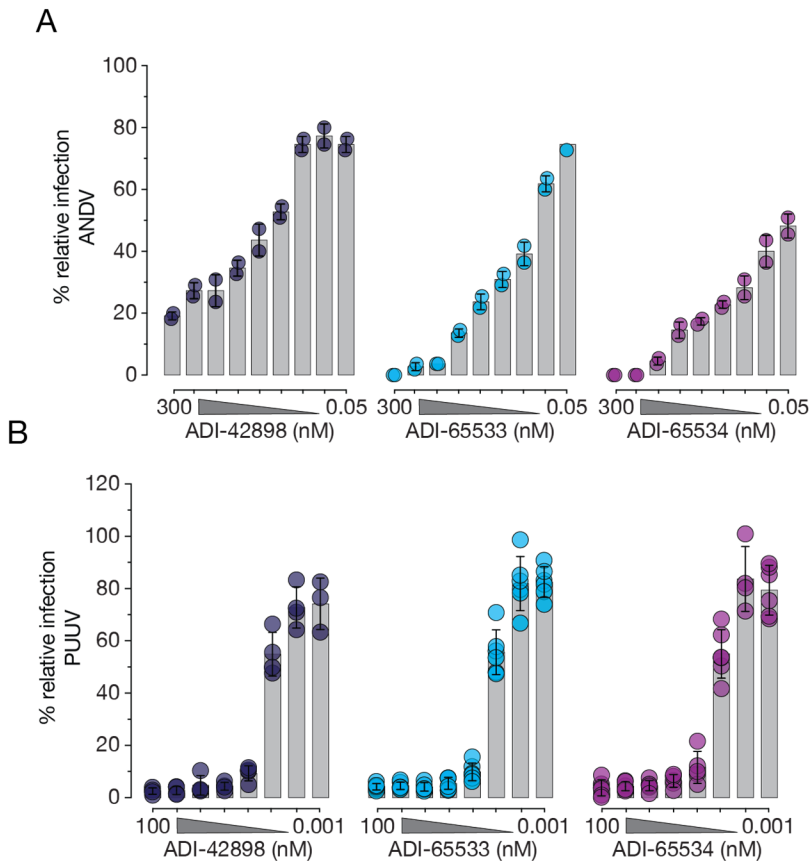


**Fig. S15. Potency of ADI-42898, ADI-65533, and ADI-65534 to block ANDV and PUUV infection.** (A) ANDV (strain Chile-7913) was exposed to 3-fold serial dilutions of the indicated mAbs starting at 300 nM; the extent of VeroE6 cell infection was determined by focus-reduction neutralization assay. Data are presented as averages  $\pm$  SD,  $n = 2$  from one experiment are shown. (B) PUUV (strain Kazan) was exposed to 5-fold serial dilutions of the indicated mAbs starting at 100 nM; the degree of Vero cell infection was determined by microneutralization assay. Data are presented as averages  $\pm$  SD,  $n = 4$  to 6 from two to three experiments are shown.

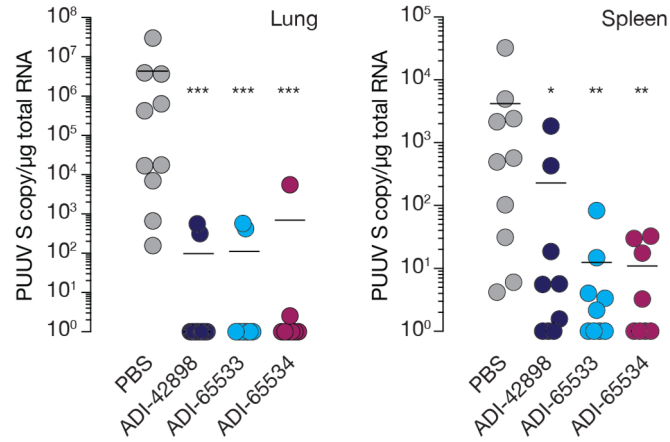


**Fig. S16. In vivo protective efficacy of human mAbs in a PUUV bank vole challenge model.** Bank voles were administered a single 5-mg/kg dose (i.p.) of the indicated mAbs or PBS vehicle ( $n = 8$  to 10 from two independent experiments), followed by a challenge with PUUV/Suo [500 FFU, subcutaneous (s.c.)] at 4 hours after mAb administration. Animals were euthanized at 3 days after challenge and organ viral RNA loads were determined by RT-qPCR detecting the PUUV S segment. Bars indicate median. Data were analyzed by an unpaired Kruskal-Wallis test comparing untreated versus mAb-treated animals; \* $P=0.0332$ ; \*\* $P=0.0021$ ; \*\*\* $P=0.0002$ .

**Table S1. Crystallographic statistics.** <sup>a</sup>data for the last resolution shell is displayed in parenthesis throughout the table; <sup>b</sup> $R_{\text{sym}} = \sum |I_i - \langle I_i \rangle| / \sum I_i$ , where  $I_i$  is the observed intensity and  $\langle I_i \rangle$  is the average intensity obtained from multiple observations of symmetry-related reflections; <sup>c</sup> $R_{\text{work}} = \sum ||F_{\text{obs}}(\text{hkl})| - |F_{\text{calc}}(\text{hkl})|| / \sum |F_{\text{obs}}(\text{hkl})|$ .

Data collection	PUUV Gn <sup>H</sup> /Gc: ADI-42898
Space group	P 2 2 <sub>1</sub> 2 <sub>1</sub>
Unit cell parameters	
<i>a</i> (Å)	83.9
<i>b</i> (Å)	109.3
<i>c</i> (Å)	149.5
$\alpha$ (°)	90
$\beta$ (°)	90
$\varphi$ (°)	90
Resolution (Å)	39.9-2.60
Last resolution bin (Å) <sup>a</sup>	2.70-2.60
Total observations	495751 (53168)
Unique reflections	43057 (4457)
Completeness (%)	100 (100)
Redundancy	11.5 (11.9)
$\langle I/s \rangle$	14.2 (0.9)
$R_{\text{sym}}$ (%) <sup>b</sup>	11.6 (276)
CC <sub>1/2</sub>	99.9 (50.3)
B Wilson (Å <sup>2</sup> )	69
<b>Refinement</b>	
PDB accession code	7QQB
Resolution (Å)	39.9-2.60
Last resolution bin (Å) <sup>a</sup>	2.63-2.60
Number of reflections	81640 (2667)
Number of reflections used to calculate R <sub>free</sub>	4029 (132)
B refinement	ISOTROPIC + TLS
Rfactor (%) <sup>c</sup>	21.2 (35.6)
R <sub>free</sub> (%)	24.9 (37.0)
Number of atoms	
shGn-Gc (A/B)	2789/3239
ADI-42898 (H/L)	950/824
Waters/glycerol	26/6
Mean B value (Å <sup>2</sup> )	
shGn-Gc (A/B)	77/85
ADI-42898 (H/L)	93/106
Waters/glycerol	64/73
Root mean square deviations	
Bond lengths (Å)	0.002
Bond angles (°)	0.505
Ramachandran favored/outliers (%)	94.55/0.2

**Data file S1. Sequences and kinetic constants of ADI-42898 variants.**  $K_D$  values of Fab fragments of ADI-42898 and 26 variants bound to ANDV and PUUV Gn<sup>H</sup>/Gc were assessed by BLI. Amino acid residues divergent from the sequence of ADI-42898 are labeled in red.

**Data file S2. Raw, individual-level data for experiments where  $n < 20$ .**